






Structure and dielectric properties of $(1-x)\text{Na}_{0.5}\text{Bi}_{0.5}\text{TiO}_3-x\text{Na}_{0.5}\text{K}_{0.5}\text{NbO}_3$ ceramics

E. V. Glazunova [§], L. A. Shilkina ^{*}, A. S. Chekhova[†], A. V. Nazarenko [‡], I. A. Verbenko ^{*}
and L. A. Reznichenko ^{*}

^{*}Research Institute of Physics, Southern Federal University
Rostov-on-Don, 344090, Russia

[†]Faculty of Physics, Southern Federal University
Rostov-on-Don, 344090, Russia

[‡]Southern Scientific Center of the Russian Academy of Sciences
Rostov-on-Don, 344006, Russia
[§]kate93g@mail.ru

Received 29 May 2023; Revised 7 September 2023; Accepted 15 October 2023; Published 4 November 2023

The solid solutions of the $(1-x)\text{Na}_{0.5}\text{Bi}_{0.5}\text{TiO}_3-x\text{Na}_{0.5}\text{K}_{0.5}\text{NbO}_3$ system were produced by the conventional ceramic technology using mechanical activation of the synthesized product. It was found that in the $(1-x)\text{Na}_{0.5}\text{Bi}_{0.5}\text{TiO}_3-x\text{Na}_{0.5}\text{K}_{0.5}\text{NbO}_3$ system at room temperature, a number of morphotropic phase transitions occur: rhombohedral \rightarrow cubic \rightarrow tetragonal \rightarrow monoclinic phases. The introduction of a small amount of $\text{Na}_{0.5}\text{K}_{0.5}\text{NbO}_3$ leads to an increase in the temperature stability of the dielectric properties of ceramics. A change in the relaxor properties of the solid solutions of the $(1-x)\text{Na}_{0.5}\text{Bi}_{0.5}\text{TiO}_3-x\text{Na}_{0.5}\text{K}_{0.5}\text{NbO}_3$ system was shown. The increase in energy density and energy efficiency was found at additive 10 mol.% of $\text{Na}_{0.5}\text{K}_{0.5}\text{NbO}_3$.

Keywords: Ceramics; lead-free materials; mechanical activation; dielectric properties; energy storage.

1. Introduction

The rapid growth of the range and functionality of small-sized electronic devices will determine the increased requirements for energy storage and processing devices. The development of ceramic capacitors for highly efficient electrical energy storage devices is of particular interest currently.^{1–3} Nowadays, the energy density in classical dielectric capacitors is insufficient to meet the ever-increasing energy consumption.^{3,4} Among the numerous materials, lead-free relaxor ferroelectrics are excellent environmentally friendly candidates for these applications due to their high intrinsic polarization and low hysteresis.^{4,6} One of the well-known and promising lead-free relaxor ferroelectric materials is ceramics based on $\text{Na}_{0.5}\text{Bi}_{0.5}\text{TiO}_3$, which has a strong intrinsic polarization, one of the reasons for which is the presence of an unshared pair of electrons Bi_{6p}^{3+} .⁷ Besides, $\text{Na}_{0.5}\text{Bi}_{0.5}\text{TiO}_3$ has a relatively high $T_C \sim 320^\circ\text{C}$, a large residual polarization, $P_r = 38 \mu\text{C}/\text{cm}^2$ and a high coercive field, $E_C = 73 \text{ kV}/\text{cm}$, as well as a high mechanical Q factor ($Q_m \sim 450$), which persists even at high exciting voltage.^{8,9}

Another promising basis for lead-free ferroelectric materials is $\text{Na}_{0.5}\text{K}_{0.5}\text{NbO}_3$ due to the relatively high Curie temperature of $\sim 420^\circ\text{C}$, as well as relatively high values of permittivity and $d_{33} \sim 200\text{--}300 \text{ pC}/\text{N}$ in doped

ceramics.^{10–14} Moreover, sodium niobate was reported to stabilize the antisegetoelectric phase of $\text{Na}_{0.5}\text{Bi}_{0.5}\text{TiO}_3$.¹⁵ It makes $\text{Na}_{0.5}\text{K}_{0.5}\text{NbO}_3$ and $\text{Na}_{0.5}\text{Bi}_{0.5}\text{TiO}_3$ promising in terms of developing materials for energy storage devices.

In the works devoted to materials based on $\text{Na}_{0.5}\text{Bi}_{0.5}\text{TiO}_3$ and $\text{Na}_{0.5}\text{K}_{0.5}\text{NbO}_3$, the outstanding properties mainly have multicomponent ceramics.^{1–5} The mechanism of formation of extreme macro-responses is not always clear due to the complex composition. Also, the reasoning for the choice of concentration range of the used components is not given. This work opens a cycle of works on the search and optimization of conditions for obtaining solid solutions based on ATiZrO_3 and ANbO_3 ($A = \text{Na, K, Bi}$) compounds with high properties of electric energy accumulation and storage.

The aim of this study is to establish the regularities of phase formation, crystal structure formation and dielectric properties of solid solutions based on $(1-x)\text{Na}_{0.5}\text{Bi}_{0.5}\text{TiO}_3-x\text{Na}_{0.5}\text{K}_{0.5}\text{NbO}_3$.

2. Subjects of Research and Methods

Solid solutions of the system $(1-x)\text{Na}_{0.5}\text{Bi}_{0.5}\text{TiO}_3-x\text{Na}_{0.5}\text{K}_{0.5}\text{NbO}_3$ ($x = 0.00; 0.10; 0.50; 0.90$) were selected as objects of research. The production of solid solutions was carried out by the method of two-stage solid-phase synthesis.

The $\text{Bi}_2\text{O}_3(99\%)*$, $\text{NaHCO}_3(99\%)*$, $\text{KHCO}_3(99\%)*$, $\text{TiO}_2(98\%)*$, $\text{Nb}_2\text{O}_5(98\%)*$ were used as raw materials (*-the content of the main component). The selection of optimal technological modes was carried out on a series of experimental samples with X-ray control of the phase composition and relative density ($\rho_{\text{rel.}}$) of the samples. The optimal synthesis modes were $T_{\text{syn1}} = (850-950)^\circ\text{C}$; $T_{\text{syn2}} = (850-970)^\circ\text{C}$; (depending on the composition) $\tau_{\text{syn1}} = \tau_{\text{syn2}} = 4$ hours; the sintering temperatures were: $T_{\text{sintering.}} = (1125 - 1150)^\circ\text{C}$ (depending on the composition), the sintering time was $\tau_{\text{sintering.}} = 2$ h. Mechanical activation (MA) was conducted before sintering using a planetary mill AGO-2. MA was carried out in alcohol for 20 min with the Zirconia balls (8 mm in diameter) as the milling media. The inner radius of the drum is 55 mm, the mass of loaded balls is 150 g for each drum, the acceleration of grinding bodies is 600 m/s^2 . The maximum rotation speed of the drums is 1820 rpm.

X-ray phase analysis is performed on a DRONE 3.0 diffractometer using $\text{CoK}\alpha$ radiation (Bragg–Brentano focusing). The calculation of the parameter a and volume V of the perovskite unit cell was carried out according to the standard methods.¹⁶ Accuracy of cell parameters determination: linear $\Delta a = \Delta c = \Delta b = \pm(0.002 - 0.004) \text{ \AA}$; angles $\Delta\alpha = \Delta\beta = \pm 0.05^\circ$; volume $\Delta V = \pm 0.05 \text{ \AA}^3$.

The experimental density (ρ_{exp}) of samples is determined by hydrostatic weighing in n -octane. The calculation of the X-ray density (ρ_{XR}) was carried out according to the following formula:

$$\rho_{\text{XR}} = \frac{M * Z}{N_A V}, \quad (1)$$

where Z is the number of the formula units, M is the molecular weight corresponding to one unit cell formula unit, N_A is the Avagadro number, V is the is the unit cell volume. The relative density (ρ_{rel}) was calculated by the following formula:

$$\rho_{\text{rel}} = \frac{\rho_{\text{exp}}}{\rho_{\text{XR}}} * 100\%. \quad (2)$$

The study of ceramic chips was carried out using a scanning electron microscope Carl Zeiss EVO 40 (Germany) in the CCP “Joint Centre of Scientific and Technological Equipment of UNC RAS (research, development, approbation)” (No 501994).

The dependences of the dielectric characteristics on temperature were obtained using the Agilent E4980A LCR meter on an automatic stand specially designed at the Research Institute of Physics with the “Kalipso” software package in the temperature range $(25-500)^\circ\text{C}$ and frequencies 1 kHz–1 MHz. The depth of the frequency dispersion of the dielectric permittivity was estimated by the following formula:

$$\Delta \varepsilon'_m = \left(\frac{\varepsilon'_{mf1} - \varepsilon'_{mf2}}{\varepsilon'_{mf1}} \right) * 100, \quad (3)$$

where ε'_{mf1} is the maximum value of $\varepsilon'/\varepsilon_0$ at the lowest frequency,

ε'_{mf2} is the maximum value of $\varepsilon'/\varepsilon_0$ at the highest frequency.

Dielectric hysteresis loops were obtained using a measuring stand assembled according to the Sawyer-Tower scheme at room temperature, a frequency of 50 Hz and an electric field value of from 700 to 2500 V for a few samples.

The energy density was obtained from the curves of the dependence of polarization on the electric field (P-E) by integrating the area between the axis of polarization and the curve P-E. With the help of integration, the values of effective energy and efficiency were calculated. The stored energy density, W_{eff} , was calculated by the following formula:

$$W_{\text{eff}} = \int_{P_r}^{P_{\text{max}}} E dP, \quad (4)$$

where P_{max} is the polarization value at maximum E , P_r is the value at $E = 0$. The values of the energy efficiency, η , were calculated by the following formula:

$$\eta = \frac{W_{\text{eff}}}{W_{\text{max}}} * 100\%. \quad (5)$$

3. Experimental Results

MA is a way to optimize conditions for obtaining ceramics and improve their properties.¹⁷ It leads to an acceleration of chemical reactions and a decrease in their temperature. In this work, MA was applied to rise the relative density of ceramics. Figure 1 shows the dependences of the solid solutions densities of the system $(1-x)\text{Na}_{0.5}\text{Bi}_{0.5}\text{TiO}_3-x\text{Na}_{0.5}\text{K}_{0.5}\text{NbO}_3$ obtained without the use of MA and with the use of MA, on temperature. It can be seen from the figure that for all x , the use of MA contributes to an increase in the density of solid solution. It is also seen that $\text{Na}_{0.5}\text{Bi}_{0.5}\text{TiO}_3$ and solid solutions, close to it, have a high density. Compositions close to $\text{Na}_{0.5}\text{K}_{0.5}\text{NbO}_3$ have $\rho_{\text{rel}} \sim 75\%$, and after MA it is possible to increase to $\sim 84\%$.

Figure 2 shows diffractograms of solid solutions of the system $(1-x)\text{Na}_{0.5}\text{Bi}_{0.5}\text{TiO}_3-x\text{Na}_{0.5}\text{K}_{0.5}\text{NbO}_3$. X-ray phase analysis of solid solutions of the system $(1-x)\text{Na}_{0.5}\text{Bi}_{0.5}\text{TiO}_3-x\text{Na}_{0.5}\text{K}_{0.5}\text{NbO}_3$ showed that all solid solutions do not contain impurities. It is established that $\text{Na}_{0.5}\text{Bi}_{0.5}\text{TiO}_3$ has rhombohedral (R) symmetry. When 10% $\text{Na}_{0.5}\text{K}_{0.5}\text{NbO}_3$ is introduced into the system, the symmetry of the solid solution changes to cubic (C). The solid solution with $x = 0.5$ also has cubic symmetry, but all diffraction peaks are double and are accompanied by modulation, which indicates spinodal decay, that is, the occurrence of two cubic phases with different cell parameters. It may be due to the fact that the electronegativity difference $\Delta\text{EN}(\text{Bi} - \text{K}) = 1.2$ is three times higher than the isomorphism conditions: the difference of ionic radii (Δr) should not exceed 15% relative to a smaller value and the electronegativity difference (ΔEN) should not exceed 0.4

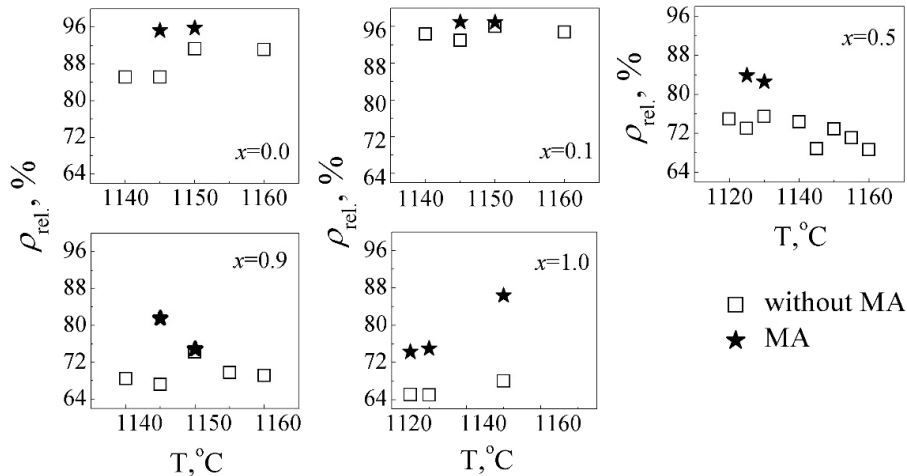


Fig. 1. Densities of solid solutions of the system $(1-x)\text{Na}_{0.5}\text{Bi}_{0.5}\text{TiO}_3-x\text{Na}_{0.5}\text{K}_{0.5}\text{NbO}_3$, obtained without MA (empty squares), and with the use of MA (colored stars).

according to Pauling.¹⁸ At $x = 0.9$, the symmetry of solid solution changes to tetragonal (T). $\text{Na}_{0.5}\text{K}_{0.5}\text{NbO}_3$ has monoclinic (M) symmetry.

Figure 2(b) shows the parameter, a , volume, V , of the unit cell and relative density of the solid solution of the $(1-x)\text{Na}_{0.5}\text{Bi}_{0.5}\text{TiO}_3-x\text{Na}_{0.5}\text{K}_{0.5}\text{NbO}_3$ system. At x increases to $x = 0.1$, the parameter and the cell volume do not change, which is caused by being close to the morphotropic transition (invar effect). In range $0.5 \leq x \leq 0.9$ the a – slightly changes and V increases noticeably, which is caused by the fact that we replace the smaller $R_{\text{Bi}^{3+}} = 1.20$ cation with the larger $R_{\text{K}^{+}} = 1.33$. In the T and M regions, only changes in the parameter a and V are considered. In range $0.9 \leq x \leq 1.0$, the a – increases and V is a little change, which is also caused by the invar effect.

The fragments of the microstructure of ceramics of the study system are shown in Fig. 3. In solid solutions with $x = 0.0$ and $x = 0.1$ a dense, almost continuous microstructure is formed. The shape of grains is close to spherical.

At $x = 0.5$ the microstructure is inhomogeneous, with chaotic loose packing of crystallites. There are both small grains $0.5 \mu\text{m}$ and less, and large grains $2-3 \mu\text{m}$. The shape of grains is predominantly cubic. When x increases further, the number of larger grains increases and the number of small grains decreases. The grain size varies $1-3 \mu\text{m}$ ($x = 0.9$). At $x = 1.0$, the grain size increases significantly to $6-10 \mu\text{m}$. The habit of grains is regular geometric shapes (parallelepipeds) resembling plate-like blocks. Thus, the behavior of the microstructure is consistent with ρ_{rel} .

The practically regular shape of grains with flat (without flaws) edges indicates that their growth, at recrystallization sintering, occurs in the presence of a liquid phase (LP), which plays the role of not so much a contact how much diffusion medium.

Thus, the increase of the crystallite size is the result of ordinary dissolution and precipitation from solution, but not the movement of interphase boundaries. The liquid covering the surface of such grains with a film forces them to acquire a

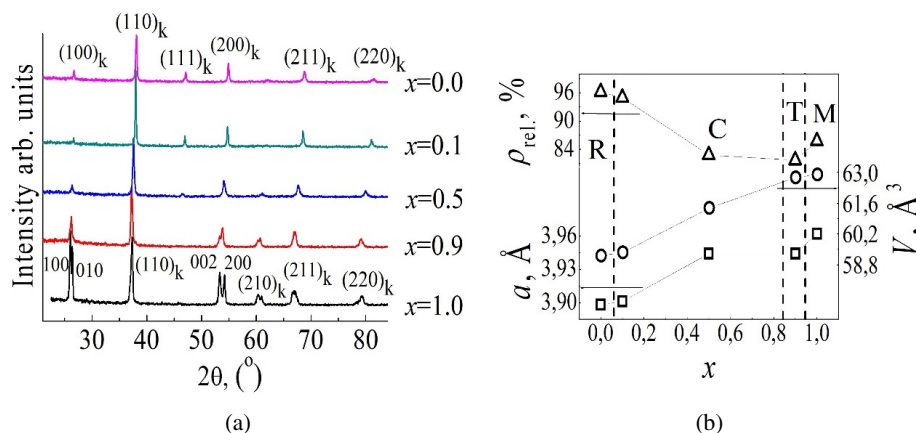


Fig. 2. Diffractograms (a) and parameter, a , and volume, V , of unit cell and relative density and (b) of solid solutions of the system $(1-x)\text{Na}_{0.5}\text{Bi}_{0.5}\text{TiO}_3-x\text{Na}_{0.5}\text{K}_{0.5}\text{NbO}_3$ after sintering.

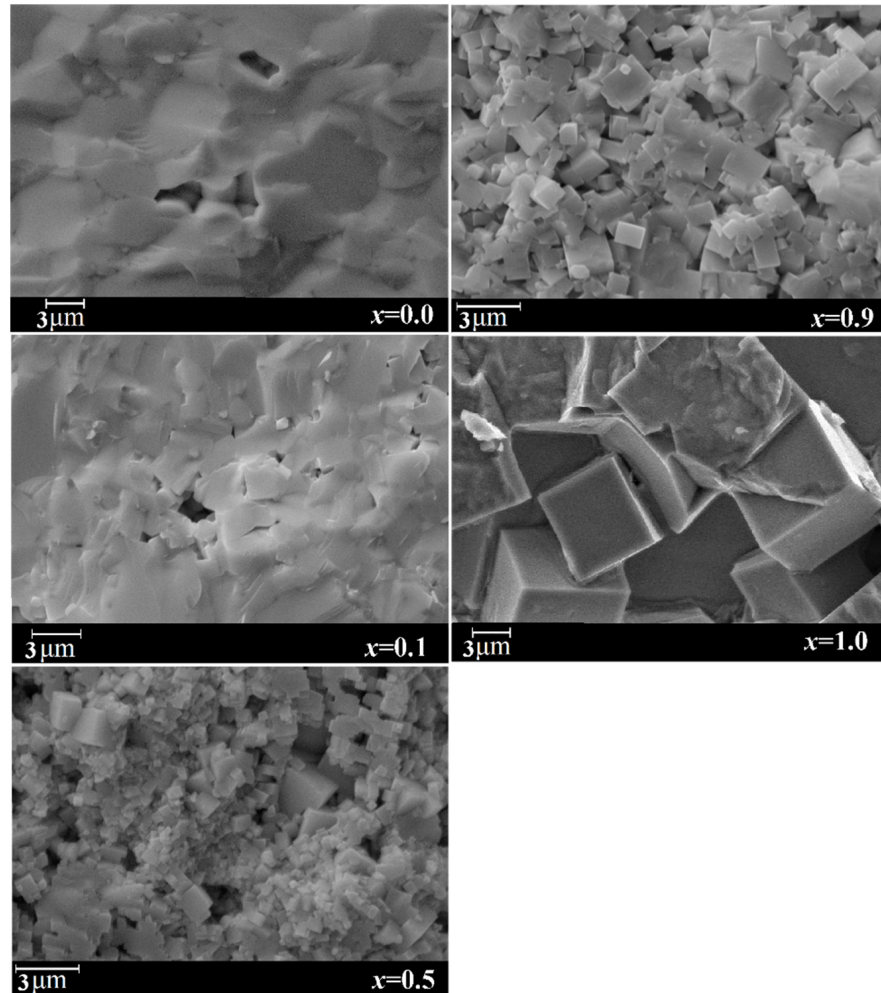


Fig. 3. Fragments of the microstructure of ceramics of the solid solutions of $(1-x)\text{Na}_{0.5}\text{Bi}_{0.5}\text{TiO}_3-x\text{Na}_{0.5}\text{K}_{0.5}\text{NbO}_3$ system.

specific growth shape and correct faceting, like the habit of crystals growing from a solution in a melt. As a result, the grains crystallize in the polyhedron's form with almost rectangular boundaries.^{19,20} The sources of LP are unreacted initial reagents, hydrolysis products, and low-melting eutectics in niobates.²⁰

Figure 4 shows the dielectric spectra of solid solutions of the system $(1-x)\text{Bi}_{0.5}\text{Na}_{0.5}\text{TiO}_3-x\text{Na}_{0.5}\text{K}_{0.5}\text{NbO}_3$ depending on the temperature in the frequency range 1 kHz–1 MHz. Analysis of the dependencies $\varepsilon_r(T)$ shows that two anomalies form in $\text{Bi}_{0.5}\text{Na}_{0.5}\text{TiO}_3$ ($x = 0.0$) at temperatures of 325°C and 180°C, which, according to the literature, relate to phase transitions from cubic to tetragonal and from tetragonal to rhombohedral phases, respectively.²¹ Introduction to the 10 mol system. % $\text{Na}_{0.5}\text{K}_{0.5}\text{NbO}_3$ ($x = 0.1$) leads to the formation of a single wide maximum on the dependence of $\varepsilon_r(T)$, shifted to the region of lower temperatures. This behavior may be due to the appearance of polar microregions, indicating that the transition to the ferroelectric state is in a higher temperature region, even though at room temperature the structure has very small distortions of the unit cell. When

add 50 mol. % $\text{Na}_{0.5}\text{K}_{0.5}\text{NbO}_3$ ($x = 0.5$), the maximum on the dependence of $\varepsilon_r(T)$ is shifted to the region of lower temperatures, below room temperature. With a further increase in the concentration of $\text{Na}_{0.5}\text{K}_{0.5}\text{NbO}_3$ to 90 mol. % ($x = 0.9$), a maximum is formed on the dependence of $\varepsilon_r(T)$ at $T_C \sim 230^\circ\text{C}$. It indicates that at $x > 0.5$ the phase transition temperature shifts again to a higher temperature region. In KNN, the dependences $\varepsilon_r(T)$ show two maxima, one sharp at $\sim 410^\circ\text{C}$,^{22,23} and the other, smeared in temperature at $T = 150\text{--}210^\circ\text{C}$, which corresponds to the phase transition from the cubic to the tetragonal phase and from tetragonal to monoclinic phase, respectively.

On the dependences of the $\varepsilon_r(T)$ at $x = 0.0$, the frequency dispersion is visible near the phase transition temperatures, $\Delta\varepsilon = 7\%$ (at 325°C). The ε_r at the maximum is 2500–2700, depending on the frequency of the electric field. At $x = 0.1$, the frequency dispersion at the time of the phase transition is not observed $\Delta\varepsilon = 2\%$ (at 220°C) but manifests itself at temperatures above and below the phase transition. At the same time, the value of ε_r decreases at the maximum to ~ 1500 degrees in the temperature range $(150\div 300)^\circ\text{C}$. At $x = 0.5$,

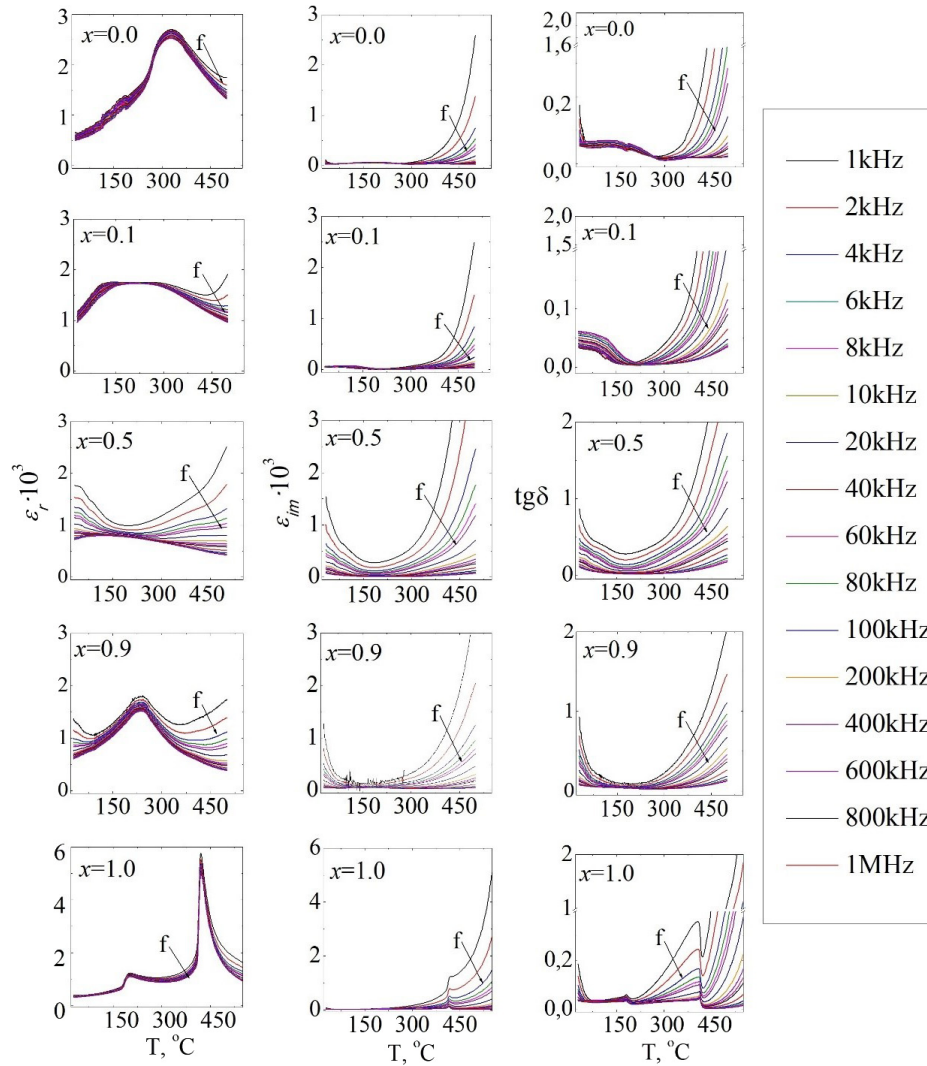


Fig. 4. Dependences of real part, ε_r , and imaginary part, ε_{im} , of the relative complex permittivity, and dielectric loss tangent, $\text{tg}\delta$, on temperature in solid solutions of the system $(1-x)\text{Na}_{0.5}\text{Bi}_{0.5}\text{TiO}_3-x\text{Na}_{0.5}\text{K}_{0.5}\text{NbO}_3$ in the frequency range 1 kHz–1 MHz (the direction of the arrow indicates an increase in frequency).

there is also a noticeable increase in the frequency dispersion of the material at temperatures above the phase transition. With a further increase in the concentration of $\text{Na}_{0.5}\text{K}_{0.5}\text{NbO}_3$ to $x = 0.9$, frequency dispersion is observed throughout the studied temperature range, $\Delta\varepsilon = 18\%$ (at 230°C). The maximum value of the ε_r is 1500–1800, depending on the frequency. The frequency dispersion in $\text{Na}_{0.5}\text{K}_{0.5}\text{NbO}_3$ frequency is $\Delta\varepsilon = 13\%$ (at 410°C). The maximum value of the ε_r is 5000–5700, depending on the frequency.

The analysis of the dependencies of $\varepsilon_{im}(T)$ and $\text{tg}\delta(T)$ demonstrates a low level of dielectric losses in these materials. A sharp increase in the analyzed values due to an increase in electrical conductivity at T above 400°C may be due to the reduction processes of $\text{Nb}^{5+} \leftrightarrow \text{Nb}^{4+}$ and $\text{Ti}^{4+} \leftrightarrow \text{Ti}^{3+}$, leading to the appearance of Maxwell–Wagner polarization.²⁴

Figure 5(a) shows the P-E hysteresis loops for solid solutions at $x = 0.0$, $x = 0.1$ at different electric fields and as an example, a comparison of loops for these solid solutions under 1900 V/cm is shown in Fig. 5(b). The experiment showed P-E hysteresis loops for $\text{Bi}_{0.5}\text{Na}_{0.5}\text{TiO}_3$ has large energy losses compared to the solid solution at $x = 0.1$. It is also shown that the applied fields do not allow reaching the saturation region in both samples.

Table 1 shows the energy density W_{eff} , energy efficiency, η , for solid solutions at $x = 0.00$, $x = 0.10$ under various electric fields.

The experiment with hysteresis loops showed that in $\text{Na}_{0.5}\text{Bi}_{0.5}\text{TiO}_3$ ($x = 0.00$) the maximum of the energy density $W_{\text{eff}} = 0.02\text{ J/cm}^3$ is observed at 1900 V with efficiency = 52%. At $x = 0.10$, the efficiency value increased noticeably. The solid solution $x = 0.10$ in the investigated

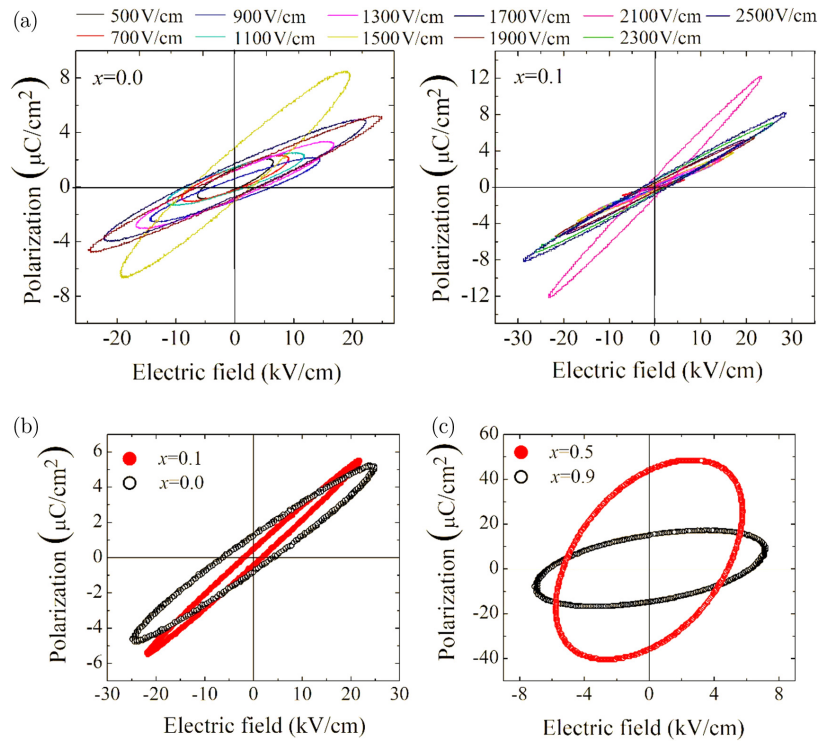


Fig. 5. P-E hysteresis loops for solid solutions at $x = 0.0$, $x = 0.1$ at different electric field (a); comparison P-E hysteresis loops for solid solutions at $x = 0.0$, $x = 0.1$ under 1900 V/cm (b); and $x = 0.5$ under 500 V/cm, and $x = 0.9$ under 900 V/cm (c).

Table 1. Energy density, energy efficiency for solid solutions at $x = 0.00$, $x = 0.10$ under various electric fields.

Concentration	Energy density	Energy efficiency
$x = 0.00$	0.02@1500 V/cm	42%
	0.01@1700 V/cm	40%
	0.02@1900 V/cm	52%
$x = 0.10$	0.01@1500 V/cm	76%
	0.02@1700 V/cm	75%
	0.03@1900 V/cm	78%
	0.06@2100 V/cm	76%
	0.04@2300 V/cm	75%
	0.05@2500 V/cm	74%

range electric field has maximum energy density $W_{\text{eff}} = 0.06 \text{ J/cm}^3$ and efficiency achieved $\eta = 76\%$ under 2100 V. At $x = 0.50$, $x = 0.90$ and $x = 1.00$, it was not possible to obtain dielectric hysteresis loops, because the solid solution has high conductivity (Fig. 5(c)). Thus, it was found that the small additive of $\text{Na}_{0.5}\text{K}_{0.5}\text{NbO}_3$ allows us an increase in energy density and efficiency.

4. Conclusions

By the method of solid-phase synthesis using MA and subsequent sintering using conventional ceramic technology,

the solid solution of systems $(1-x)\text{Na}_{0.5}\text{Bi}_{0.5}\text{TiO}_3-x\text{Na}_{0.5}\text{K}_{0.5}\text{NbO}_3$ was obtained.

A number of morphotropic phase transitions occur in the $(1-x)\text{Na}_{0.5}\text{Bi}_{0.5}\text{TiO}_3-x\text{Na}_{0.5}\text{K}_{0.5}\text{NbO}_3$ system at room temperature: rhombohedral \rightarrow cubic \rightarrow tetragonal \rightarrow monoclinic phases were found.

The temperature stability of dielectric properties was found in the range $(150\div 300)^\circ\text{C}$ while maintaining low values of $\text{tg}\delta$ in this temperature range at the addition of 10 mol. % $\text{Na}_{0.5}\text{K}_{0.5}\text{NbO}_3$. At 2100 V/cm, the maximum energy density and energy efficiency have a solid solution with $x = 0.1$, $W_{\text{eff}} = 0.06 \text{ J/cm}^3$ and $\eta = 76\%$.

5. Summary

Thus, in solid solutions of the $(1-x)\text{Na}_{0.5}\text{Bi}_{0.5}\text{TiO}_3-x\text{Na}_{0.5}\text{K}_{0.5}\text{NbO}_3$ obtained electrical properties that exceed the characteristics of the extreme components of the system, signifying their application potential in energy storage devices and necessitating further studies to determine the compositions, which have optimal electrophysical properties, as well as their study in higher electric fields.


Acknowledgments

The study was carried out with the financial support of the Ministry of Science and Higher Education of the Russian


Federation (State task in the field of scientific activity in 2023). Project No. FENW-2023-0010/(GZ0110/23-11-IF). using the equipment of the Center for Collective Use “Electromagnetic, Electromechanical and Thermal properties of Solids” of the Research Institute of Physics of the Southern Federal University.


ORCID

E. V. Glazunova  <https://orcid.org/0000-0002-2596-2471>

L. A. Shilkina  <https://orcid.org/0000-0002-8048-3617>

A. V. Nazarenko  <https://orcid.org/0000-0001-9684-693X>

I. A. Verbenko  <https://orcid.org/0000-0001-6229-9691>

L. A. Reznichenko  <https://orcid.org/0000-0001-5202-1610>

References

- L. Yang, X. Kong, F. Li, H. Hao, Z. Cheng, H. Liu, J.-F. Li and S. Zhang, Perovskite Lead-free dielectrics for energy storage applications, *Prog. Mater. Sci.* **102**, 72 (2019), doi: 10.1016/j.pmatsci.2018.12.005.
- B. Xu, J. Iniguez and L. Bellaiche, Designing lead-free antiferroelectrics for energy storage, *Nat. Commun.* **8**, 15682 (2017), doi: 10.1038/ncomms15682.
- G. Wang, Z. Lu, Y. Li, L. Li, H. Ji, A. Feteira, D. Zhou, D. Wang, S. Zhang and I. M. Reaney, Electroceramics for high-energy density capacitors: Current status and future perspectives, *Chem. Rev.* **121**, 6124 (2021), doi: 10.1021/acs.chemrev.0c01264.
- K. Zou, Y. Dan, H. Xu et al., Recent advances in lead free dielectric materials for energy storage, *Mater. Res. Bull.* **113**, 190 (2019), doi: 10.1016/j.materresbull.2019.02.002.
- X. Zhou, G. Xue a, H. Luo, C. R. Bowen and D. Zhang, Phase structure and properties of sodium bismuth titanate lead-free piezoelectric ceramics, *Prog. Mater. Sci.* **122**, 100836 (2021), doi: 10.1016/j.pmatsci.2021.100836.
- N. Kumar, A. Ionin, T. Ansell, S. Kwon, W. Hackenberger and D. Cann, Multilayer ceramic capacitors based on relaxor BaTiO₃-Bi(Zn_{1/2}Ti_{1/2})O₃ for temperature stable and high energy density capacitor applications, *Appl. Phys. Lett.* **106**, 252901 (2015), doi: 10.1063/1.4922947.
- T. Li, P. Chen, F. Li and C. Wang, Energy storage performance of Na_{0.5}Bi_{0.5}TiO₃ SrTiO₃ lead-free relaxors modified by AgNb_{0.85}Ta_{0.15}O₃, *Chem. Eng. J.* **406**, 127151 (2021), doi: 10.1016/j.cej.2020.127151.
- F. Yan, K. Huang, T. Jiang, X. Zhou, Y. Shi, G. Ge, B. Shen and J. Zhai, Significantly enhanced energy storage density and efficiency of BNT-based perovskite ceramics via A-site defect engineering, *Energy Storage Mater.* **30**, 392 (2020), doi: 10.1016/j.ensm.2020.05.026.
- H. Hu, M. Zhu, F. Xie, N. Lei, J. Chen, Y. Hou and H. Yan, Effect of Co₂O₃ additive on structure and electrical properties of 85 (Bi_{1/2}Na_{1/2})TiO₃-12(Bi_{1/2}K_{1/2})TiO₃-3BaTiO₃ lead-free piezoceramics, *J. Am. Ceram. Soc.* **92**(9), 2039 (2009), doi: 10.1111/j.1551-2916.2009.03183.x.
- Q. Zhou, Z. Peng, F. Zhang, Q. Chai, D. Wu, P. Liang, L. Wei, X. Chao and Z. Yang, Achieving high comprehensive energy storage properties of BNT-based ceramics via multiscale regulation, *Ceram. Int.* **49**(12), 19701 (2023), doi: 10.1016/j.ceramint.2023.03.087.
- H. Birol, D. Damjanovic and N. Setter, Preparation and characterization of (K_{0.5}Na_{0.5})NbO₃ ceramics, *J. Eur. Ceram.* **26**(6), 861 (2006), doi: 10.1016/j.jeurceramsoc.2004.11.022.
- R. Zuo, J. Rodel, R. Chen and L. Li, Sintering and electrical properties of lead-free Na_{0.5}K_{0.5}NbO₃ piezoelectric ceramics, *J. Am. Ceram. Soc.* **89**(6), 2010 (2006), doi: 10.1111/j.1551-2916.2006.00991.x.
- R. Hu, Y. Lin, M. Zhang, Q. Yuan and H. Yang, Enhancement of recoverable energy density and efficiency of Na_{0.5}K_{0.5}NbO₃ ceramic modified by Bi(Mg_{0.5}Zr_{0.5})O₃, *Mater. Today Energy* **30**, 101185 (2022), doi: 10.1016/j.mtener.2022.101185.
- X. Peng, B. Yang, D. Deng, Z. Cai, X. Kong, L. Yang and J. Guo, Lead-free KNN-based ceramics incorporated with Bi (Zn_{2/3}Nb_{1/3})O₃ possessing excellent optical transmittance and superior energy storage density, *Mater. Res. Bull.* **165**, 112294 (2023), doi: 10.1016/j.materresbull.2023.112294.
- H. Qi and R. Zuo, Linear-like lead-free relaxor antiferroelectric (Bi_{0.5}Na_{0.5})TiO₃-NaNbO₃ with giant energy-storage density/efficiency and super stability against temperature and frequency, *J. Mater. Chem. A* **7**, 3971 (2019), doi: 10.1039/c8ta12232f.
- E. G. Fesenko, *The Perovskite Family and Ferroelectricity* (Atomizdat, 1972).
- Z. Di et al., Nanopowder preparation and dielectric properties of a Bi₂O₃-Nb₂O₅ binary system prepared by the high-energy ball-milling method, *J. Am. Ceram. Soc.* **91**, 139 (2008), doi: 10.1111/J.1551-2916.2007.02017.X.
- C. N. R. Rao and J. Gopalakrishnan, *New Directions in Solid State Chemistry* (Cambridge University Press, Cambridge, 1986).
- W. D. Kingery, *Introduction to Ceramics* (Publishing House of Literature on Construction, 1967).
- L. A. Reznichenko, G. A. Geguzina and N. V. Dergunova, Piezoelectric solid solutions based on alkali niobates, *Inorganic Materials* **34**(2), 167 (1998).
- J. Yin, Y. Zhang, X. Lv and J. Wu, Ultrahigh energy-storage potential under low electric field in bismuth sodium titanate-based perovskite ferroelectrics, *J. Mater. Chem. A* **6**, 9823 (2018), doi: 10.1039/c8ta00474a.
- B. Jaffe, W. R. Cook and H. Jaffe, *Piezoelectric Ceramics* (Academic Press, London, 1971).
- J.-F. Li, K. Wang, F.-Y. Zhu, L.-Q. Cheng and F.-Z. Yao, (K,Na) NbO₃-based lead-free piezoceramics: Fundamental aspects, processing technologies, and remaining challenges, *J. Am. Ceram. Soc.* **96**, 3677 (2013), doi: 10.1111/jace.12715.
- G. G. Vezzoli, Electrical properties of NbO₂ and Nb₂O₅ at elevated temperature in air and flowing argon, *Phys. Rev. B* **26**(7), 3954 (1982), doi: 10.1103/PHYSREVB.26.3954.